The SDSS-XMM Quasar Sample: First Results

Guido Risaliti[1,2] & Martin Elvis[1]

`grisaliti@cfa.harvard.edu`

ABSTRACT

We have searched in the *XMM-Newton* public archive for quasars in the Sloan Digital Sky Survey (SDSS) First Data Release (DR1), and found 55 lying in the field of a *XMM-Newton* observation with exposure times >20 ksec (as of August, 2004). The 35 quasars which yielded good X-ray spectra span redshifts from 0.5 to 2.5. The large collecting area of *XMM-Newton* allows us to investigate the dependence of the X-ray spectra of quasars on luminosity, redshift and optical colors. We find: (1) no evolution of X-ray slope (Γ) with either redshift or luminosity; (2) no correlation between Γ or absorbing column density and the optical to X-ray ratio, α_{OX}; (4) no relation between α_{OX} and optical colors. The two latter results suggest that obscuration is not the dominant cause of the spread in X-ray slope or optical color. We find four unusual quasars, 10% of the sample: three are absorbed ($N_H > 10^{22} \text{cm}^{-2}$), of which one has high luminosity ($1.5 \times 10^{44} \text{erg s}^{-1}$); the fourth has $\Gamma = 0.6 \pm 0.2$, far flatter than the typical value of 1.8-2.0, and a strong emission line (EW=1.2 ± 0.4 keV) which, if Fe-K, implies a redshift of ~ 1.4.

Subject headings: Galaxies: AGN — X-rays: galaxies

1. Introduction

Surveys of the X-ray properties of optically selected quasars have followed two main lines:
(1) detailed spectral analysis of relatively small samples (≤ 30) of bright, mostly low redshift objects (Elvis et al. 1987, Laor et al. 1997, George et al. 2000, Reeves & Turner 2000), primarily using the Bright Palomar Survey ($B < 16.3$) ("PG", Schmidt & Green 1983).

[1]Harvard-Smithsonian Center for Astrophysics, 60 Garden St. Cambridge, MA 02138 USA

[2]INAF - Osservatorio Astrofisico di Arcetri, L.go E. Fermi 5, Firenze 05125 Italy

These works have shown that radio quiet quasars have on average a power-law spectrum in the X-rays, with photon index $\Gamma \sim 2$, analogous to what is found for the lower luminosity Seyfert 1 Galaxies (George et al. 1998, Perola et al. 2002), and are not absorbed, with the exception of Broad Absorption Line (BAL) quasars, which represent $\sim 10 - 20\%$ of optically selected objects (Reichard et al. 2003).

(2) statistical investigations of large (~ 100) samples using only X-ray fluxes, in order to compare X-ray and optical/UV properties (Zamorani et al. 1981, Avni & Tananbaum 1986, Wilkes et al. 1994, Yuan et al. 1998, Bechtold et al. 2003, Vignali, Brandt & Schneider 2003, hereinafter V03, Strateva et al. 2005). These works have clearly established a relation between the X-ray to optical ratio with optical luminosity: more luminous objects are X-ray fainter (relatively to the optical emission).

What has not been possible is a study of the X-ray spectra of a large sample of quasars, especially one spanning a wide range of luminosity and redshift. Hence a change in X-ray loudness might be due to a change of the intrinsic continuum production method or efficiency, or merely to line of sight obscuration (Risaliti et al. 2001).

The new generation optical surveys and X-ray instruments are changing this situation significantly: the Sloan Digital Sky Survey (SDSS, York et al. 2000) will provide high quality optical spectra and photometry for $\sim 100,000$ quasars spanning a redshift interval from 0 to > 6.

The expected X-ray flux of SDSS quasars can be estimated from optical magnitudes assuming the median standard Spectral Energy Distribution (SED) of Elvis et al. (1994) and the luminosity - α_{OX} relation of V03. They range from $\sim 10^{-14}$ to $\sim 10^{-13}$ erg s^{-1} cm^{-2}, accessible to *Chandra* (Weisskopf et al. 2002) and *XMM-Newton* (Jansen et al. 2001) for good quality X-ray spectra (>100-1000 counts). Pointed observations with both the X-ray observatories have been performed for the highest redshift ($z > 4$) SDSS quasars (Brandt et al. 2002, Bechtold et al. 2003, Vignali et al. 2003a,b).

To obtain large samples of X-ray spectra for lower redshift SDSS quasars targetted observations are less efficient than a 'serendipitous' approach. *XMM-Newton* has larger collecting area ($\sim 1,800$ cm^2 at 2 keV, vs. ~ 400 cm^2) and field of view (a circle of $\sim$14 arcmin radius, vs $\sim$8 arcmin) than *Chandra*. A source with a standard radio-quiet quasar spectrum and 2-10 keV flux of 10^{-14} erg s^{-1} cm^{-2} observed by XMM will give a ~ 100 counts in $\sim$10 ksec.

Here we present the results of a first analysis of the X-ray properties of 55 SDSS quasars serendipitously observed by *XMM-Newton* in long (> 20 ksec) observations. The quasars

span redshifts from 0.5-2.5 and a wide range of luminosities. The SDSS selection criteria (Richards et al. 2002) are based on the locus of quasars in a multi-color space, and allows the selection of objects redder than the classical UV-excess selected objects (e.g. Schmidt & Green 1983). As a consequence, a significant fraction ($\sim 10\%$) of optically red quasars is present in the SDSS (Richards et al. 2003). We first investigate the relations between X-ray properties and luminosity , redshift and optical colors. We then concentrate on the analysis of four objects with peculiar X-ray properties. Finallly, we briefly discuss the expected quality of the final sample.

2. The SDSS - XMM-Newton DR1-04 Quasar Sample

As of August 2004, of the 18,650 quasars of the SDSS DR1, the *XMM-Newton* public archive[1] contained 150 within 14' of the XMM optical axis, which are not the main targets of the XMM observations. The length of the XMM observations varies between $\sim$4 ksec and $\sim$100 ksec.

We extracted the XMM data for the 58 quasars in the 20 longest *XMM-Newton* observations (> 20 ksec). For each object we extracted the spectra from the two EPIC CCD detectors PN and MOS (from the combined MOS1 and MOS2 observations). In 15 cases the object was found to lie in a bad region in one of the two instruments, either in a strip between two adjacent chips, or in a zone outside the field of view (in particular, the PN instrument has a rectangular shape, therefore our circular selection region does not overlap at large distances [$> 10'$] from the on-axis position). For these 15 objects we performed our analysis using the only available detector. In 3 cases ($\sim 5\%$) the quasar lay a bad region in both the observations, therefore no XMM spectrum is available. For the remaining 40 cases both the PN and MOS spectra are available. For five quasars only a flux measurement was possible due to the low S/N, while 15 others are not detected. For these objects we estimated a flux upper limit, based on the effective observation length and on the off-axis distance. For the 35 remaining objects we extracted and analyzed the X-ray spectrum. For all 35 well-detected sources, the background was extracted from a region of the same observation at the same off-axis distance as the source.

---

[0]We estimate luminosity distances using the standard "concordance" cosmological parameter $(h_0, \Omega_M, \Omega_\lambda) = (0.7, 0.3, 0.7)$, Spergel et al. 2003.

[1]URL: http://xmm.vilspa.esa.es

3. First results

In order to obtain homogeneous results, we fitted all the 0.5-10 keV spectra with a simple model of a power law (of photon index Γ) absorbed by an intrinsic column density (N_H), and the Galactic column density from the maps collected by Dickey & Lockman (1990). We used XSPEC V.11.3 (Arnaud 1996) as the fitting engine, and the standard χ^2 minimization technique, after rebinning in order to have at least 15 counts per spectral channel. The largest Galactic column density toward these high Galactic latitude objects is $7 \times 10^{20} \mathrm{cm}^{-2}$, and is typically $2\text{-}3 \times 10^{20} \mathrm{cm}^{-2}$.

The main results of the X-ray spectral and correlation studies are shown in Figures 1 and 2. First we note that previous studies were mainly based either on low-redshift objects, like the PG quasars, or on upper limits on the X-ray flux for objects with $z > 1$, while our sources homogeneously sample the $\sim$0.5-2.5 redshift range (Fig. 1a), with a detection rate which is high ($\sim 70\%$) and constant with redshift up to $z \sim 2.5$ (Fig. 1b).

The XMM results are consistent with the VO3 α_{OX} - luminosity correlation (Fig. 1c), and the lack of correlation between α_{OX} and redshift (Fig. 1d). The main new results are the following:

1. No spectral evolution with luminosity or redshift has been found. The photon index is on average consistent with values $\Gamma = 1.8-2$ (Fig. 2a and 2b), typical of low luminosity, low redshift AGNs (George et al. 2000, Mineo et al. 2000). Since the rest frame energy range changes substantially with redshift, reaching above 30 keV for the three z>2 quasars, all of which have well determined Γ values, we conclude that quasar spectral slopes are unchanged up to $\sim$30 keV.

2. No correlation is present between Γ and the B-R color (Fig. 2c). This implies that the X-ray index and optical colors are driven by different physical parameters, not by obscuration. This is expected e.g. in a disk-corona scenario (e.g. Haardt & Maraschi 1991), where the optical-UV slope is determined by the physical conditions in the accretion disk, while the slope of the X-ray emission is related to the temperature and Compton depth of the hot corona.

3. Γ is not related to α_{OX} (Fig. 2d). The implication is that the *efficiency* of X-ray production relative to the optical (accretion disk) power is separate from the *mechanism* that determines the spectral shape of the X-ray emission. Moreover, the spread in α_{OX} cannot be due to absorption, because then flatter spectra would be found in X-ray weak objects.

4. The scatter around the α_{OX}-optical luminosity relation does not depend on optical color. In Fig. 1e we plot the difference $\Delta\alpha_{0X}$ between the measured α_{OX} and the one expected based on the V03 relation, versus the optical color B-R. No correlation is present. If red optical colors were due to reddening by cold material then red objects would be X-ray weak due to absorption. The lack of correlation suggests that on average the X-ray loudness of quasars and the optical colors are driven by different physical processes, and are not related to absorption/extinction.

5. All but three quasars show no low-energy photoelectric cut-off ($N_H < 10^{22}$cm^{-2}, Fig. 1f). Since all these quasars are type 1 objects (i.e. have broad optical emission lines) this is not surprising as such objects are typically unobscured. The three exceptions are the three reddest objects, with (B-R)>1 (Fig. 2c) and are discussed below.

3.1. Unusual quasars

Four of the 35 quasars with XMM X-ray spectra ($\sim 10\%$ of the sample) have properties that clearly diverge from the rest.

Three of them are obscured by a column density $N_H > 10^{22}$ cm^{-2}. Of these, two (SDSS J033718.81+003303.7, z=0.437, and SDSS J09345834+6112343, z=0.245, marked as #1 and #2 in the figures) are high-z analogs of Narrow Emission Line Galaxies (Ward et al. 1978) in the local Universe: they have optical spectra of type 1.8-1.9 Seyferts, an X-ray column density of $N_H = 1.3^{+0.5}_{-0.8} \times 10^{22}$ cm^{-2} and $N_H = 2.6^{+1.8}_{-0.9} \times 10^{22}$ cm^{-2}, respectively, and moderate 2-10 keV luminosities, $\sim 10^{43}$ erg s^{-1}.

The third object (SDSS J030238.16+000203.4, z=1.35, marked as #3 in the figures) is more unusual, in having an optical spectrum typical of a blue broad line quasar (FWHM(MgII,CIII])$\sim$ $4,000$ km s^{-1}), with an X-ray spectrum absorbed by an intrinsic column density $N_H = 2.5^{+1.2}_{-0.9} \times 10^{22}$ cm^{-2}. The intrinsic 2-10 keV luminosity is 1.5×10^{44} erg s^{-1}. The absorber is significantly more dust-free than normal in AGNs, with an upper limit for the dust to gas ratio $\sim 1/50$ of the Galactic value, compared to typical AGN values of $\sim 1/10$ (Maccacaro, Perola & Elvis 1982, Maiolino et al. 2001). These properties make this object one of the few known high redshift X-ray absorbed quasars.

The fourth interesting object is the only one with a spectral index significantly flatter than the average (SDSS J093533.01+612738.6, $\Gamma = 0.6 \pm 0.2$, Fig. 2, marked as #4 in the figures). This object is classified as a z=0.475 quasar. However, there are no clear spectral lines in the SDSS spectrum, and the X-ray spectrum, in addition to a flat continuum, shows a strong emission line (EW=1.2±0.4 keV) consistent with an iron Kα line at z$\sim$ 1.4 (Fig. 3).

If confirmed, this would be one of the few high redshift Compton thick AGNs (e.g. Norman et al. 2002), and a rare case of a redshift being first determined in X-rays.

3.2. Predicted final SDSS-XMM sample

We used the results obtained above to estimate the properties and size of the SDSS-XMM sample once all the SDSS spectra are released, assuming just the current 5 years of XMM operations. For each of the sources of the intial sample of 150 objects (Sect. 2) which we did not analyze directly, we estimated the expected S/N taking into account the mirror vignetting, the average background counts, the probability of a non-detection due to a bad position in one or both detectors, and the probability of background flares affecting part of the observations.

In Table 1 we present the statistics obtained for the first 55 objects (numbers in parentheses), and that expected for the final SDSS-XMM quasar sample. We divided the sources in 5 quality groups, according to the measured (for the 55 objects with X-ray analysis) or expected (for the other objects) S/N: (1) S/N>25: sources for which a relatively detailed spectral analysis is possible; (2) 10<S/N<25: sources for which a basic spectral analysis (power law continuum, absorption) can be performed; (3) 5<S/N<10: only a single component can be fitted (equivalent to a hardness ratio measurement); (4) 2<S/N<5: only a flux measurement can be obtained; (5) non-detection: an upper limit of the flux can be estimated. We also show the expected distribution in redshift.

These numbers will increase as XMM observes longer. A reasonable estimate is that at the time the full SDSS quasar sample is released (early 2006) the XMM public archive will be 30-40% larger than at the time we performed our search. The total number of SDSS quasars with *XMM-Newton* detections will then approach 1,000.

4. Conclusions

We have cross-correlated the SDSS DR1 quasar sample with the *XMM-Newton* public archive, and found 150 SDSS objects that were serendipitously observed by XMM. We estimate that over half of these objects will have a good enough spectrum (S/N>10) in order to estimate the basic spectral parameters (observed 0.5-10 keV photon index, Γ, intrinsic photoelectric absorption, N_H). In this paper we presented the analysis of the XMM spectra of 55 of these quasars observed in long (>20 ksec) *XMM-Newton* observations. The quality of the data fully confirms our expectations.

We find that most SDSS quasars have spectral properties analogous to those of bright PG quasars, with a small spread in Γ, and no evolution of Γ with redshift (z) or luminosity. As there are three quasars with well-determined Γ at $z > 2$, we conclude that quasar spectra have no change in slope up to $\sim$30 keV. We also find that the X-ray photon index (Γ) is independent from X-ray loudness (α_{OX}), so that the efficiency of X-ray production in quasar appears to be independent from the details of the mechanism of X-ray production. No correlation is found between α_{ox} and optical colors, suggesting that the observed spread in the X-ray to optical ratio is not related to obscuration.

Four of the 35 sources, 10% of the sample, have unusual X-ray spectra. The three optically reddest objects in our sample (B-R>1) are also those that show significant intrinsic X-ray absorbing column density. Their SDSS spectra show two to be type 1.8-1.9 Seyferts, while one is an optically normal unreddened quasar, yet with $N_H \sim$2-3$\times 10^{22}$ cm^{-2}, suggesting the presence of a dust-free absorber. One object shows a reflection-dominated X-ray spectrum, and possibly belongs to the elusive class of high-z, Compton-thick AGNs.

The work presented here is a first part of a large project. When the final SDSS quasar sample becomes available, over 700 quasars will have XMM observations. An analysis of the recently released DR3 sample (Abazajian et al. 2005) is on-going, and will include correlations between the X-ray spectra and the SDSS optical spectral properties.

REFERENCES

Abazajian, K., et al. 2005, AJ, 129, 1755

Brandt, W. N., et al. 2002, ApJ, 569, L5

Dickey, J. M., & Lockman, F. J. 1990, ARA&A, 28, 215

Elvis, M., et al. 1994, ApJS, 95, 1

George, I. M., Turner, T. J., Netzer, H., Nandra, K., Mushotzky, R. F., & Yaqoob, T. 1998, ApJS, 114, 73

George, I. M., et al. 2000, ApJ, 531, 52

Haardt, F., & Maraschi, L. 1991, ApJ, 380, L51

Jansen, F., et al. 2001, A&A, 365, L1

Laor, A., Fiore, F., Elvis, M., Wilkes, B. J., & McDowell, J. C. 1997, ApJ, 477, 93

Maccacaro, T., Perola, G. C., & Elvis, M. 1982, ApJ, 257, 47

Maiolino, R., Marconi, A., Salvati, M., Risaliti, G., Severgnini, P., Oliva, E., La Franca, F., & Vanzi, L. 2001, A&A, 365, 28

Mineo, T., et al. 2000, A&A, 359, 471

Norman, C., et al. 2002, ApJ, 571, 218

Perola, G. C., Matt, G., Cappi, M., Fiore, F., Guainazzi, M., Maraschi, L., Petrucci, P. O., & Piro, L. 2002, A&A, 389, 802

Reeves, J. N. & Turner, M. J. L. 2000, MNRAS, 316, 234

Reichard, T. A., et al. 2003, AJ, 126, 2594

Richards, G. T., et al. 2002, AJ, 123, 2945

Richards, G. T., et al. 2003, AJ, 126, 1131

Risaliti, G., Marconi, A., Maiolino, R., Salvati, M., & Severgnini, P. 2001, A&A, 371, 37

Schmidt, M., & Green, R. F. 1983, ApJ, 269, 352

Spergel, D. N., et al. 2003, ApJS, 148, 175

Strateva, I, Brandt, W. N., Schneider, D. P., Vanden Berk, D. G., & Vignali, C. 2005, ApJ, accepted (astro-ph/0503009)

Vignali, C., et al. 2003, AJ, 125, 2876

Vignali, C., Brandt, W. N., Schneider, D. P., Garmire, G. P., & Kaspi, S. 2003a, AJ, 125, 418

Vignali, C., Brandt, W. N., & Schneider, D. P. 2003b, AJ, 125, 433

Ward, M. J., Wilson, A. S., Penston, M. V., Elvis, M., Maccacaro, T., & Tritton, K. P. 1978, ApJ, 223, 788

Weisskopf, M. C., Brinkman, B., Canizares, C., Garmire, G., Murray, S., & Van Speybroeck, L. P. 2002, PASP, 114, 1

Wilkes, B. J., Tananbaum, H., Worrall, D. M., Avni, Y., Oey, M. S., & Flanagan, J. 1994, ApJS, 92, 53

York, D. G., et al. 2000, AJ, 120, 1579

Yuan, W., Brinkmann, W., Siebert, J., & Voges, W. 1998, A&A, 330, 108

Zamorani, G., et al. 1981, ApJ, 245, 357

Table 1: SDSS-XMM Sample Distribution

z→ S/N↓	< 0.5	0.5-1	1-1.5	1.5-2	>2	Σ_z	Σ_z^{cum}
>25	(0)5	(4)26	(0)5	(2)10	(2)15	(8)61	61
10-25	(3)50	(4)77	(8)107	(7)87	(1)10	(23)331	392
5-10	(1)5	(1)26	(1)51	(0)87	(1)57	(4)226	618
2-5	(0)5	(2)5	(1)15	(1)10	(1)15	(5)50	668
<2	(2)5	(4)26	(4)21	(4)21	(1)15	(15)88	756
$\Sigma_{S/N}$	(6)70	(15)160	(14)199	(14)215	(6)112	(55)756	
$\Sigma_{S/N}^{cum}$	70	230	429	644	756		

Number of sources in a given interval of redshift and S/N in the 0.5-10 keV band (from the combined MOS+PN instruments). Numbers in parentheses refer to the sample of 55 sources analyzed in this paper. The other numbers are our predictions for the final SDSS-XMM sample. The last line contains the cumulative number of quasars up to the indicated redshift. Similarly, the last column shows the cumulative number of spectra with a S/N higher than the indicated value.
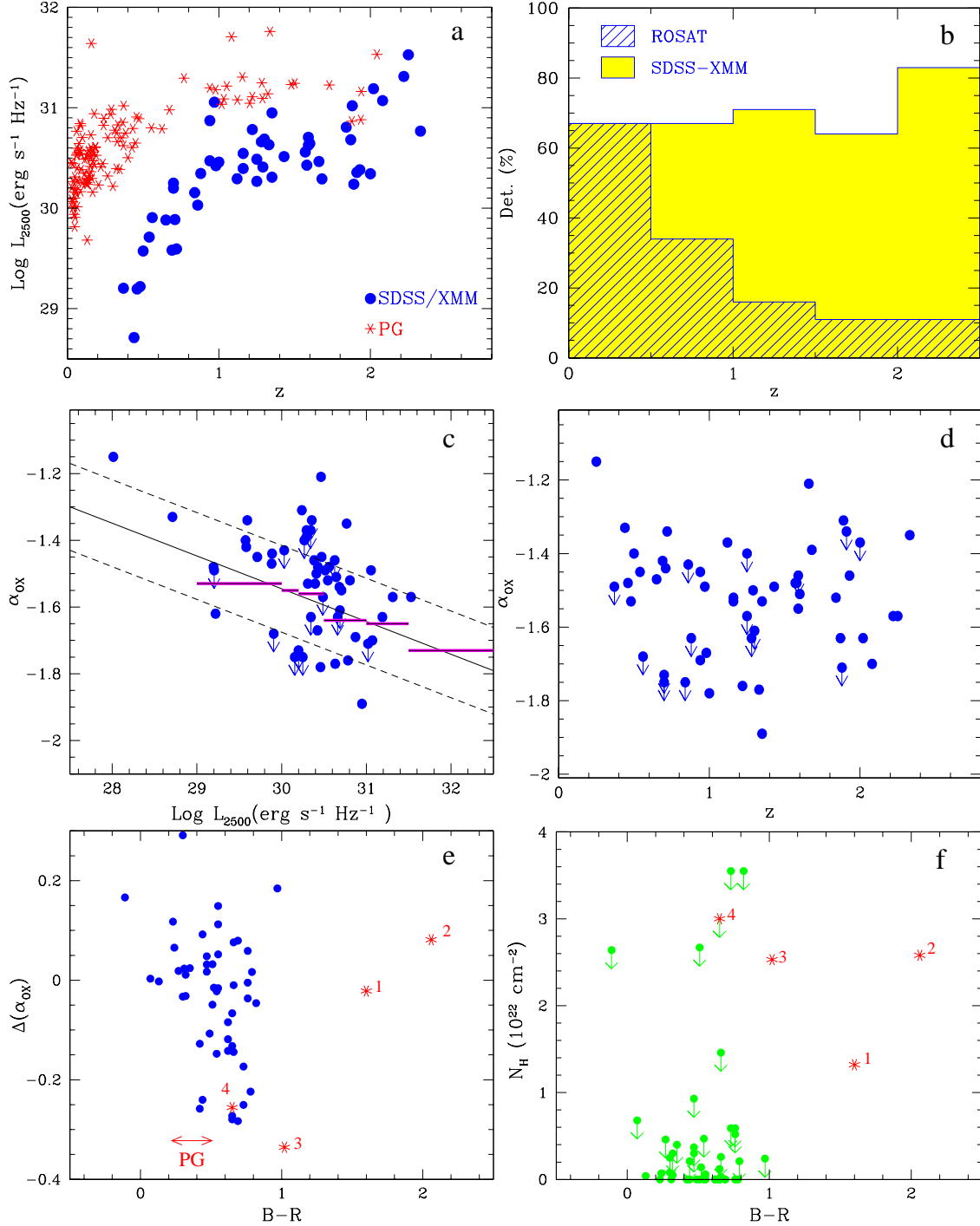
Fig. 1.— Results of X-ray analysis and correlation with optical properties for the SDSS-XMM sample. **a**: Luminosity-redshift plot for our sample, compared with that of PG quasars. **b**: Fraction of detected sources versus redshift for our sample and the one of Yuan et al. (1998). **c** and **d**: X-ray photon index versus optical 2500 Å monochromatic luminosity and versus redshift. In the first plot, our data are compared with the correlation inferred by V03 (continuous thick line, with the two dashed lines indicating the statistical errors, and with the correlation by Yuan et al. 1998 (horizontal segments). **e**: Residuals of the measured α_{OX} with respect to the V03 relation, versus optica B-R color. **f**: N_H versus B-R color. The four peculiar objects discussed in Section 3.1 are marked as stars.
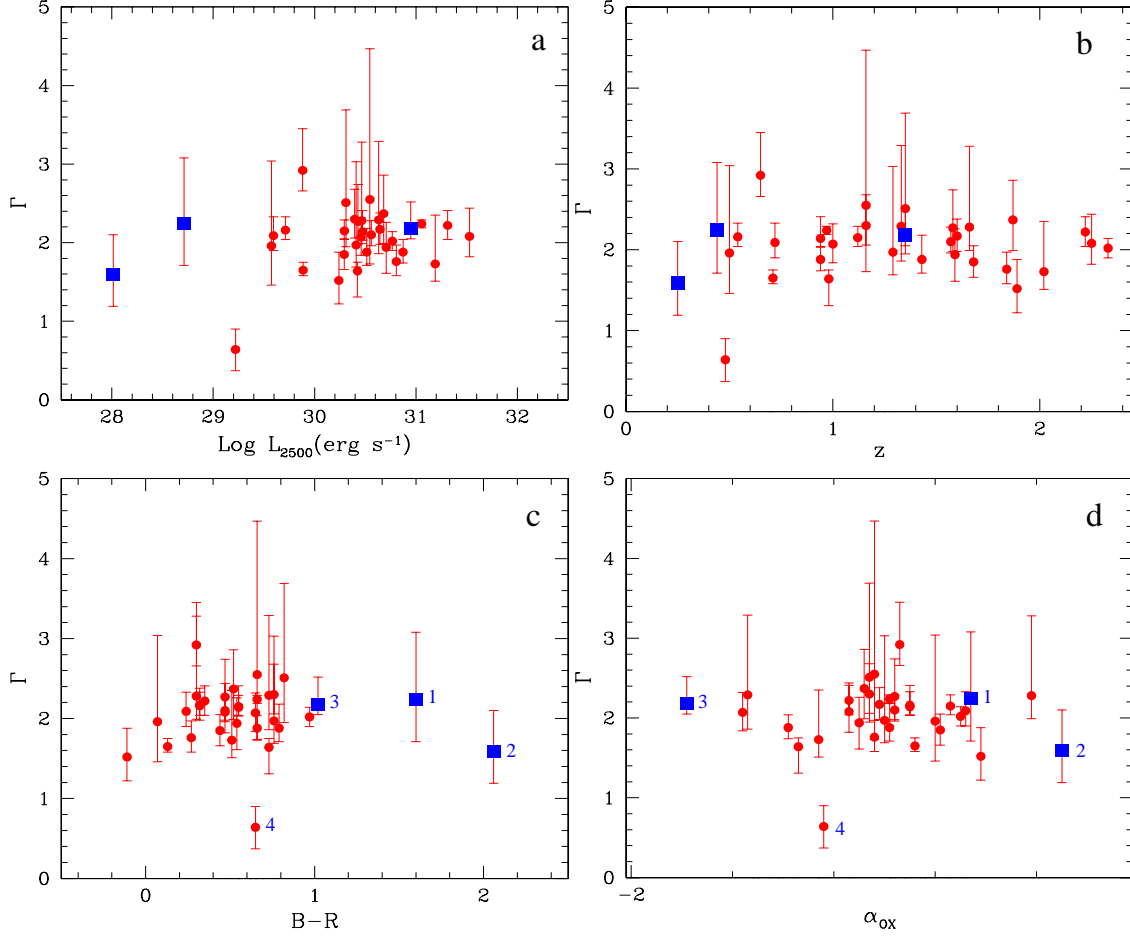
Fig. 2.— X-ray photon index versus **a**: optical 2500 Å monochromatic luminosity; **b**: red-shift; **c**: B-R color; **d**: α_{OX}. The three squares are for the "peculiar" quasars with a measured column density $N_H > 10^{22}$ cm^{-2}.
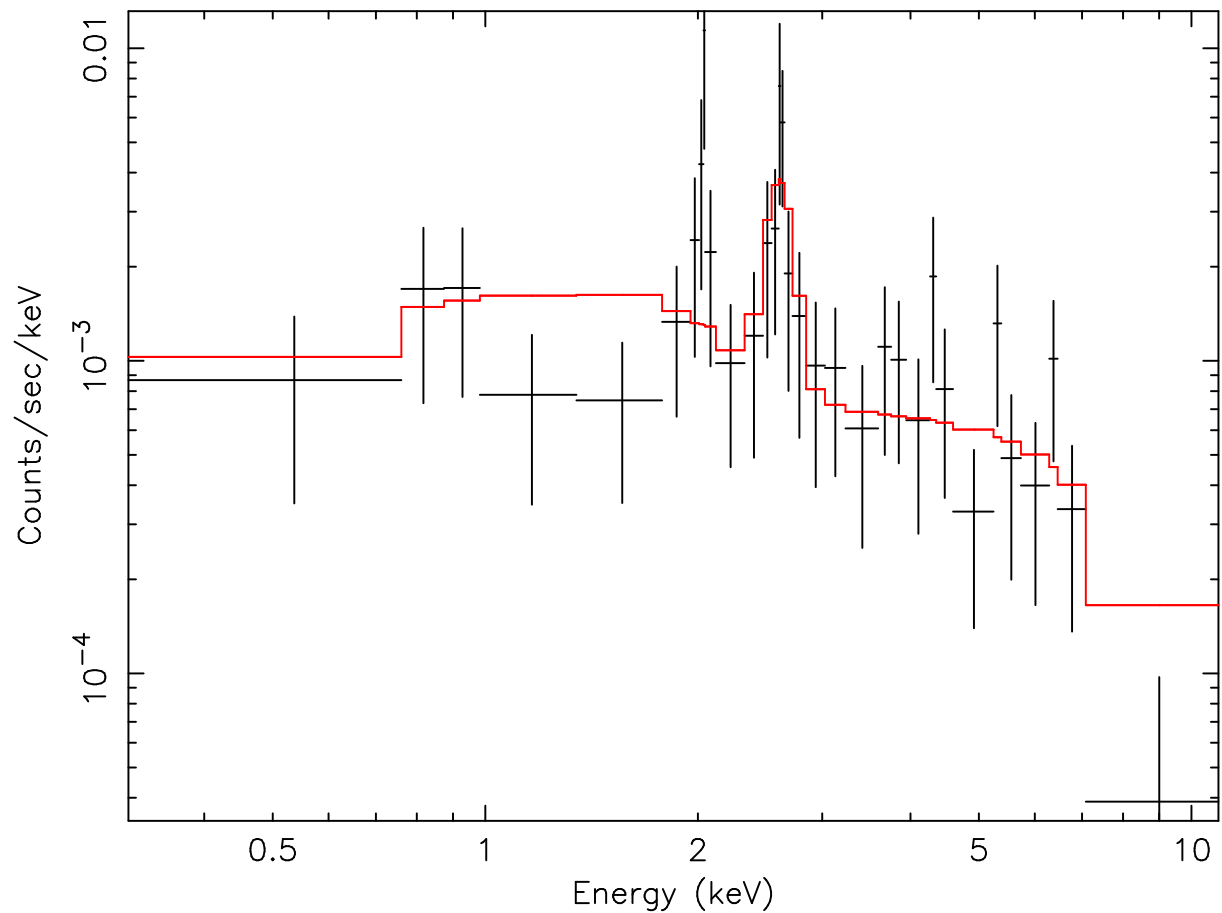
Fig. 3.— X-ray spectrum of the object marked as #4. Both the flat continuum ($\Gamma \sim 0.7$) and the putative iron line (4σ excess, with EW~ 1.2 keV) point to a reflection dominated, $z \sim 1.4$ quasar
.